

## Characteristic of Stress Distribution at a Vertex in Orthotropic Piezo-ceramic Bi-material Bonded Joints

Md. ShahidulIslam<sup>1</sup>, and A. T. M. Mashud<sup>2</sup>

<sup>1</sup> Professor, Dept. of Mechanical Engineering, Khulna University of Engineering & Technology, Bangladesh

<sup>2</sup> Dept. of Mechanical Engineering, Khulna University of Engineering & Technology, Khulna-9203, Bangladesh  
shahidulbitk@gmail.com\* and masud.an19@gmail.com

**Abstract**-Material science and simulation is getting popular for its cost benefit ratio. With the development of new materials and replacing old costly material with the new one is going to help the next generation technology of smart material. Simulation provides a better way for the test as it only requires enough processing power of the computer to finish the calculation. It is less expensive than the real test but can give almost accurate results to predict the future of the tests. Piezo-ceramic material has gained more attention in recent years for their properties and huge application in sensors and transducers. So it is of great importance to know how piezoelectric material behaves under mechanical stress especially when they are bonded with another one. Many researchers have been investigated the characteristic of stress field in piezo-ceramic boned joints. But the stress concentration near the vertex of interface in bonded joint is not clear until now. In this paper, characteristic of stress distribution at a vertex of interface is investigated using eigen analysis based on Finite Element Method (FEM). From the simulation result, it is observed that the high stress concentration occurs near the vertex of interface in orthotropic piezo-ceramic bi-material Bonded Joints.

**Keywords:** Piezo-ceramics, Orthotropic, FEM, Eigen Analysis, and Bi-material

### 1. INTRODUCTION

In the material science, piezoelectric materials have drawn attention in the recent years due to its properties. Piezoelectricity is the electric charge that accumulates in certain solid materials such as crystals, certain ceramics, and biological matter such as bone, DNA and various proteins in response to applied mechanical stress. For its property it is widely used for transducer and sensor [1].

A piezoelectricsensor is a device that uses the piezoelectric effect, to measure changes in pressure, acceleration, temperature, strain or force by converting them to an electrical charge. When pressure or force changes, electricity generate and by calibrating them to a known value it are useful to use them as sensor. A transducer is any device used to convert energy from one form to another; typically when converting input energy into output energy. For transduction to occur, a change from one form of energy must also take place, such as a conversion from mechanical to electrical energy or vice versa [2].

During deformation, Piezo-electric material produces significant amount of electricity to affect its different behavior. So different piezo-electric and di-electric properties are included in the analysis. Adhesive bonding has been increasingly used in joining and repairing load-carrying structural components because of its characteristics. Generally adhesive bond is

lighter than any other, more uniform and efficient load transfer into the patch and can reduce the risk of high stress concentrations. This leads to the wide use of bonded repairs instead of using riveted repairs in aircraft structures. One of the common examples of bonded joint is the single step butt joint or T-joint. Existing single step joints are made of two substrates joined by using the mechanical connection method, chemical connection method or solid phase bonding process [3].

When two piezo-ceramic materials are joined together and placed under a tensile force, a high stress concentration occurs near the vertex of the joints. Many researchers have been investigated the effect of stress field in piezo-ceramic boned joints. But the characteristics of stress concentration near the vertex of interface are not clear until now. In this paper, characteristic of stress distribution at a vertex of interface in bonded joints is investigated using eigen analysis based on FEM. The eigen equation is used for investigating the order of stress singularity and the angular function of elastic displacement, electric potential, stress and electric displacement.

### 2. FORMULA OF ANALYSIS

In the absence of body forces and free charges, the equilibrium equations of piezoelectric materials are expressed as follows [4]:

$$\sigma_{ij,j} = 0, \quad d_{i,i} = 0. \quad (1)$$

The constitutive relations are shown as follows:

$$\sigma_{ij} = c_{ijkl}\varepsilon_{kl} - e_{kij}E_k, \quad d_i = e_{ikl}\varepsilon_{kl} + \chi_{ik}E_k. \quad (2)$$

The elastic strain-displacement and electric field-potential relations are presented as follows:

$$\varepsilon_{ij} = \frac{1}{2}(u_{j,i} + u_{i,j}), \quad E_i = -\psi_{,i} \quad (3)$$

where  $i, j, k, l = 1, 2, 3$  and  $\sigma_{ij}, d_i, \varepsilon_{ij}, u_i, E_i,$  and  $\psi$  are the component of stress, electric displacement, strain, elastic displacement, electric field and electric potential respectively.

For orthotropic material, the constructive relation is expressed in the following form.

$$\{\sigma\} = [c]\{\varepsilon\} - [e]\{E\}, \quad \{d\} = [e]\{\varepsilon\} + [\chi]\{E\} \quad (4)$$

In Cartesian coordinate the constitutive equation reduced to the matrix form as follows.

$$\begin{Bmatrix} \sigma_{11} \\ \sigma_{22} \\ \sigma_{33} \\ \sigma_{23} \\ \sigma_{31} \\ \sigma_{12} \end{Bmatrix} = \begin{bmatrix} c_{11} & c_{12} & c_{13} & 0 & 0 & 0 \\ c_{12} & c_{22} & c_{23} & 0 & 0 & 0 \\ c_{13} & c_{23} & c_{33} & 0 & 0 & 0 \\ 0 & 0 & 0 & c_{44} & 0 & 0 \\ 0 & 0 & 0 & 0 & c_{55} & 0 \\ 0 & 0 & 0 & 0 & 0 & c_{66} \end{bmatrix} \begin{Bmatrix} \varepsilon_{11} \\ \varepsilon_{22} \\ \varepsilon_{33} \\ 2\varepsilon_{23} \\ 2\varepsilon_{31} \\ 2\varepsilon_{12} \end{Bmatrix}$$

$$- \begin{bmatrix} 0 & 0 & e_{31} \\ 0 & 0 & e_{32} \\ 0 & 0 & e_{33} \\ 0 & e_{24} & 0 \\ e_{15} & 0 & 0 \\ 0 & 0 & 0 \end{bmatrix} \begin{Bmatrix} E_1 \\ E_2 \\ E_3 \end{Bmatrix} \quad (5)$$

$$\begin{Bmatrix} d_1 \\ d_2 \\ d_3 \end{Bmatrix} = \begin{bmatrix} 0 & 0 & 0 & 0 & e_{15} & 0 \\ 0 & 0 & 0 & e_{24} & 0 & 0 \\ e_{31} & e_{32} & e_{33} & 0 & 0 & 0 \end{bmatrix} \begin{Bmatrix} \varepsilon_{11} \\ \varepsilon_{22} \\ \varepsilon_{33} \\ 2\varepsilon_{23} \\ 2\varepsilon_{31} \\ 2\varepsilon_{12} \end{Bmatrix}$$

$$- \begin{bmatrix} \chi_{11} & 0 & 0 \\ 0 & \chi_{22} & 0 \\ 0 & 0 & \chi_{33} \end{bmatrix} \begin{Bmatrix} E_1 \\ E_2 \\ E_3 \end{Bmatrix} \quad (6)$$

The combined form of Eq. (4) is expressed as follows.

$$\begin{Bmatrix} \sigma \\ d \end{Bmatrix} = \begin{Bmatrix} c \\ e \end{Bmatrix}^T \begin{Bmatrix} \varepsilon \\ -E \end{Bmatrix} = \{D\} \begin{Bmatrix} \varepsilon \\ -E \end{Bmatrix} = \{D\} \{\varepsilon^*\} \quad (7)$$

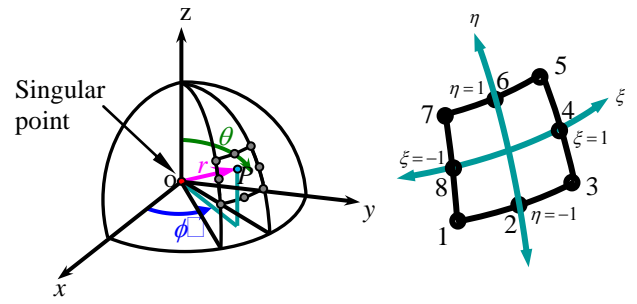


Fig.1: Element geometry and natural co-ordinates at a free edge singular point

Figure1 represents the geometry of a typical case where a singular stress state occurs at the point o. The region surrounding the singular point is divided into a number of quadratic pyramidal elements with a summit o, with each element being located in spherical co-ordinates  $r, \theta$  and  $\phi$  by its nodes 1 to 8. A point  $P$  in the element can be located using the singular transformation by the following relations [4].

$$r = r_o \left( \frac{1+\alpha}{2} \right)^{1/P} \quad \text{or,} \quad \rho = \frac{r}{r_o} \left( \frac{1+\alpha}{2} \right)^{1/P} \quad (8)$$

$$\theta = \sum_{i=1}^8 H_i \theta_i \quad \text{and} \quad \phi = \sum_{i=1}^8 H_i \phi_i \quad (9)$$

Where  $\rho$  eigen value,  $\rho = r/r_o$ ,  $r$  the distance from the singular point, and  $H_i$  indicates the shape function, which is written as;

$$H_1 = -\frac{1}{4}(1-\eta)(1-\xi)(\eta+\xi+1), \quad H_2 = \frac{1}{2}(1-\eta)(1-\xi^2)$$

$$H_3 = -\frac{1}{4}(1-\eta)(1+\xi)(-\eta+\xi-1), \quad H_4 = \frac{1}{2}(1-\eta^2)(1+\xi)$$

$$H_5 = \frac{1}{4}(1+\eta)(1+\xi)(\eta+\xi-1), \quad H_6 = \frac{1}{2}(1+\eta)(1-\xi^2)$$

$$H_7 = \frac{1}{4}(1+\eta)(1-\xi)(\eta-\xi-1), \quad H_8 = \frac{1}{2}(1-\eta^2)(1-\xi)$$

$\theta$  and  $\phi$  are the nodal values of the angular co-ordinates and  $\alpha, \eta,$  and  $\xi$  are natural co-ordinates of the element whose ranges are shown in Fig.1.

The elastic displacement and electric potential field in the element is expressed as follows:

$$\begin{aligned} (\bar{u} - \bar{u}_o) &= \left( \frac{1+\alpha}{2} \right) \left[ \sum_{i=1}^8 H_i (\bar{u}_i - \bar{u}_o) \right] \\ (\bar{\psi} - \bar{\psi}_o) &= \left( \frac{1+\alpha}{2} \right) \left[ \sum_{i=1}^8 H_i (\bar{\psi}_i - \bar{\psi}_o) \right] \end{aligned} \quad (10)$$

where  $\bar{u}_o$  and  $\bar{u}$  is the elastic displacement at o and  $P$ , respectively, and  $\bar{\psi}_o$  and  $\bar{\psi}$  is the electric potential at o and  $P$ , respectively. In order to simplify the notation, the following equation can be defined.

$$\begin{aligned} u &= (\bar{u} - \bar{u}_o), \quad u_i = (\bar{u}_i - \bar{u}_o) \quad \text{and} \\ \psi &= (\bar{\psi} - \bar{\psi}_o), \quad \psi_i = (\bar{\psi}_i - \bar{\psi}_o) \end{aligned} \quad (11)$$

Using the Eq. (8), Eq. (10) can be expressed as follows:

$$\begin{aligned} u_k &= \rho^P \left[ \sum_{i=1}^8 H_i u_{ki} \right] \quad \text{where } k = r, \theta, \phi, \quad \text{and} \\ \psi &= \rho^P \left[ \sum_{i=1}^8 H_i \psi_i \right] \end{aligned} \quad (12)$$

The Jacobian matrix relating the spherical coordinates to the natural coordinates is given below:

$$[\mathbf{J}] = \begin{bmatrix} \frac{\partial r}{\partial \alpha} & \frac{\partial \theta}{\partial \alpha} & \frac{\partial \phi}{\partial \alpha} \\ \frac{\partial r}{\partial \xi} & \frac{\partial \theta}{\partial \xi} & \frac{\partial \phi}{\partial \xi} \\ \frac{\partial r}{\partial \eta} & \frac{\partial \theta}{\partial \eta} & \frac{\partial \phi}{\partial \eta} \end{bmatrix} = \begin{bmatrix} \frac{r_o}{2P} \rho^{1-P} & 0 & 0 \\ 0 & \sum_{i=1}^8 H_{i,\xi} \theta_i & \sum_{i=1}^8 H_{i,\xi} \phi_i \\ 0 & \sum_{i=1}^8 H_{i,\eta} \theta_i & \sum_{i=1}^8 H_{i,\eta} \phi_i \end{bmatrix} \quad (13)$$

Eq. (13) shows that there is no dependence between the radial coordinate and the angular coordinate. From Eq. (13) a sub-matrix is extracted as follows:

$$[\mathbf{J}_1] = \begin{bmatrix} \frac{\partial \theta}{\partial \xi} & \frac{\partial \phi}{\partial \xi} \\ \frac{\partial \theta}{\partial \eta} & \frac{\partial \phi}{\partial \eta} \end{bmatrix} = \begin{bmatrix} \sum_{i=1}^8 H_{i,\xi} \theta_i & \sum_{i=1}^8 H_{i,\xi} \phi_i \\ \sum_{i=1}^8 H_{i,\eta} \theta_i & \sum_{i=1}^8 H_{i,\eta} \phi_i \end{bmatrix} \quad (14)$$

The strain and electric potential equation is obtained from Eqs. (8), (9) and Eqs. (12), (14) by using the chain rule of differentiation. The strain in a spherical coordinate system [1]:

$$\begin{aligned} \varepsilon_{rr} &= \frac{\partial u_r}{\partial r} = \frac{p\rho^{P-1}}{r_o} \left[ \sum_{i=1}^8 H_i u_{ri} \right] \\ \varepsilon_{\theta\theta} &= \frac{\partial u_\theta}{r \partial \theta} = \frac{\rho^{P-1}}{r_o} \left\{ \sum_{i=1}^8 H_i u_{ri} + [J_1(1,1)]^{-1} \left[ \sum_{i=1}^8 \frac{\partial H_i}{\partial \xi} u_{\theta i} \right] \right. \\ &\quad \left. + [J_1(1,2)]^{-1} \left[ \sum_{i=1}^8 \frac{\partial H_i}{\partial \eta} u_{\theta i} \right] \right\} \end{aligned}$$

$$\begin{aligned} \varepsilon_{\phi\phi} &= \frac{u_\theta}{r} \cot \theta + \frac{1}{r \sin \theta} \frac{\partial u_\phi}{\partial \phi} + \frac{u_r}{r} \\ &= \frac{\rho^{P-1}}{r_o} \left\{ \sum_{i=1}^8 H_i u_{ri} + \cot \theta \left[ \sum_{i=1}^8 H_i u_{\theta i} \right] \right\} \end{aligned}$$

$$+ \frac{[J_1(2,1)]^{-1}}{\sin \theta} \left[ \sum_{i=1}^8 \frac{\partial H_i}{\partial \xi} u_{\phi i} \right] + \frac{[J_1(2,2)]^{-1}}{\sin \theta} \left[ \sum_{i=1}^8 \frac{\partial H_i}{\partial \eta} u_{\phi i} \right] \quad (15)$$

$$\begin{aligned} \gamma_{\theta\phi} &= \frac{1}{r \sin \theta} \frac{\partial u_\theta}{\partial \phi} + \frac{\partial u_\phi}{r \partial \theta} - \frac{u_\phi}{r} \cot \theta \\ &= \frac{\rho^{P-1}}{r_o} \left\{ -\cot \theta \sum_{i=1}^8 H_i u_{\phi i} + [J_1(1,1)]^{-1} \left[ \sum_{i=1}^8 \frac{\partial H_i}{\partial \xi} u_{\phi i} \right] \right. \\ &\quad \left. + [J_1(1,2)]^{-1} \left[ \sum_{i=1}^8 \frac{\partial H_i}{\partial \eta} u_{\phi i} \right] \right\} \end{aligned}$$

$$+ \frac{[J_1(2,1)]^{-1}}{\sin \theta} \left[ \sum_{i=1}^8 \frac{\partial H_i}{\partial \xi} u_{\theta i} \right] + \frac{[J_1(2,2)]^{-1}}{\sin \theta} \left[ \sum_{i=1}^8 \frac{\partial H_i}{\partial \eta} u_{\theta i} \right]$$

$$\gamma_{r\phi} = \frac{1}{r \sin \theta} \frac{\partial u_r}{\partial \phi} + \frac{\partial u_\phi}{\partial r} - \frac{u_\phi}{r} = \left( \frac{\rho^{p-1}}{r_o} \right) \left\{ (p-1) \left[ \sum_{i=1}^8 H_i u_{\phi i} \right] \right.$$

$$+ \frac{[J_1(2,1)]^{-1}}{\sin \theta} \left[ \sum_{i=1}^8 \frac{\partial H_i}{\partial \xi} u_{ri} \right] + \frac{[J_1(2,2)]^{-1}}{\sin \theta} \left[ \sum_{i=1}^8 \frac{\partial H_i}{\partial \eta} u_{ri} \right] \left. \right\}$$

$$\gamma_{r\theta} = \frac{\partial u_r}{r \partial \theta} + \frac{\partial u_\theta}{\partial r} - \frac{u_\theta}{r} = \left( \frac{\rho^{p-1}}{r_o} \right) \left\{ (p-1) \left[ \sum_{i=1}^8 H_i u_{\theta i} \right] \right.$$

$$+ [J_1(1,1)]^{-1} \left[ \sum_{i=1}^8 \frac{\partial H_i}{\partial \xi} u_{ri} \right] + [J_1(1,2)]^{-1} \left[ \sum_{i=1}^8 \frac{\partial H_i}{\partial \eta} u_{ri} \right] \quad (15)$$

(12)

The electric potential in a spherical coordinate system:

$$E_r = -\frac{\partial \psi}{\partial r} = -\left( \frac{p\rho^{P-1}}{r_o} \right) \left[ \sum_{i=1}^8 H_i \psi_i \right]$$

$$\begin{aligned} E_\theta &= -\frac{\partial \psi}{r \partial \theta} = -\left( \frac{\rho^{P-1}}{r_o} \right) \left\{ [J_1(1,1)]^{-1} \left[ \sum_{i=1}^8 \frac{\partial H_i}{\partial \xi} \psi_i \right] \right. \\ &\quad \left. + [J_1(1,2)]^{-1} \left[ \sum_{i=1}^8 \frac{\partial H_i}{\partial \eta} \psi_i \right] \right\} \end{aligned}$$

$$\begin{aligned} E_\phi &= -\frac{1}{r \sin \theta} \frac{\partial \psi}{\partial \theta} = -\left( \frac{\rho^{P-1}}{r_o} \right) \left\{ \frac{[J_1(2,1)]^{-1}}{\sin \theta} \left[ \sum_{i=1}^8 \frac{\partial H_i}{\partial \xi} \psi_i \right] \right. \\ &\quad \left. + \frac{[J_1(2,2)]^{-1}}{\sin \theta} \left[ \sum_{i=1}^8 \frac{\partial H_i}{\partial \eta} \psi_i \right] \right\} \quad (16) \end{aligned}$$

The superscript -1 on the matrix  $[\mathbf{J}_1]$  represents the inverse matrix. Eqs. (15) and (16) now can be summarized as follows:

$$\left\{ \varepsilon^* \right\} = \sum_{i=0}^8 [\mathbf{B}_i] \left\{ \mathbf{u}_i^* \right\} = [\mathbf{B}] \left\{ \mathbf{u}^* \right\} \quad (17)$$

Where

$$\{\boldsymbol{\varepsilon}^*\}^T = \{\varepsilon_{rr} \quad \varepsilon_{\theta\theta} \quad \varepsilon_{\phi\phi} \quad \varepsilon_{r\theta} \quad \varepsilon_{r\phi} \quad \varepsilon_{\theta\phi} \quad E_r \quad E_\theta \quad E_\phi\}$$

$$\{\mathbf{u}_i^*\}^T = \{\bar{u}_{ri} \quad \bar{u}_{\theta i} \quad \bar{u}_{\phi i} \quad -\bar{\psi}_i\}$$

$$[\mathbf{B}] = \frac{1}{r_o} \rho^{p-1} (p[\mathbf{B}_a] + [\mathbf{B}_b])$$

Eq.(17) represents the strains, and therefore the stresses are proportional to  $\rho^{p-1}$ . The case where  $0 < p < 1$  defines a singular stress state at the vertex of the element. The element depicted in Fig.1 must satisfy the principle of virtual work in order to be in equilibrium, that is

$$\int_{\Omega} \sigma_{ij}^* \delta \varepsilon_{ij}^* d\Omega = \int_{\Gamma} T_i^* \delta u_i^* d\Gamma + \int_{\Omega} f_i^* \delta u_i^* d\Omega \quad (18)$$

Where  $T_i^*$  represents the traction at the outer boundary. This equation can be transformed into a matrix form with the help of Eqs. (8) and (9) as follows:

$$\int_{-1}^1 \int_{-1}^1 \int_{r_o}^1 \rho^2 \left( \delta \{\boldsymbol{\varepsilon}^*\}^T \{\boldsymbol{\sigma}^*\} \right) \sin \theta |\mathbf{J}| d\alpha d\xi d\eta$$

$$= \int_{-1}^1 \int_{-1}^1 \int_{r_o}^1 \delta \{\mathbf{u}^*\}^T \{\mathbf{H}\}^T \begin{Bmatrix} \sigma_{rr} \\ \sigma_{r\phi} \\ \sigma_{r\theta} \\ d_r \end{Bmatrix} \sin \theta |\mathbf{J}_1| d\xi d\eta \quad (19)$$

Where  $|\mathbf{J}|$  and  $|\mathbf{J}_1|$  represent the determinant of the matrices  $[\mathbf{J}]$  and  $[\mathbf{J}_1]$  respectively and  $\{\boldsymbol{\sigma}^*\}^T$  is represented by the following equation.

$$\{\boldsymbol{\sigma}^*\}^T = \{\sigma_{rr} \quad \sigma_{\theta\theta} \quad \sigma_{\phi\phi} \quad \sigma_{r\theta} \quad \sigma_{r\phi} \quad \sigma_{\theta\phi} \quad d_r \quad d_\theta \quad d_\phi\} \quad (20)$$

The relation between stress and electric displacement with strain and electric field is as follows:

$$\{\boldsymbol{\sigma}^*\} = [\mathbf{D}] \{\boldsymbol{\varepsilon}^*\} \quad (21)$$

where  $\mathbf{D}$  represents the material constants matrix.

The  $9 \times 9$  matrix  $[\mathbf{D}]$  is expressed in the spherical coordinate system. The matrix  $[\mathbf{D}]$  is evaluated at each Gauss point during the numerical evaluation of the integrals. The material properties in the rectangular coordinate system  $(x, y, z)$  are transformed to the spherical coordinate system  $(r, \theta, \phi)$ . Where  $r, \theta,$  and  $\phi$  represent the spherical coordinates of any Gauss point.

The eigen equation was formulated for determining the order of stress singularity as follows [5]:

$$(p^2 [\mathbf{A}] + p [\mathbf{B}] + [\mathbf{C}]) \{\mathbf{U}\} = \{0\} \quad (22)$$

where  $\{\mathbf{U}\} = \begin{Bmatrix} u_r \\ u_\theta \\ u_\phi \\ \psi \end{Bmatrix}$

$$[\mathbf{A}] = \sum_s ([\mathbf{k}_a - \mathbf{k}_{sa}]), [\mathbf{B}] = \sum_s ([\mathbf{k}_b - \mathbf{k}_{sb}]),$$

$$[\mathbf{C}] = \sum_s ([\mathbf{k}_c - \mathbf{k}_{sc}])$$

In Eq. (22)  $p$  represents the characteristic root, which is related to the order of singularity,  $\lambda$ , as  $\lambda = 1 - p$ .  $[\mathbf{A}]$ ,  $[\mathbf{B}]$  and  $[\mathbf{C}]$  are matrices composed of material properties, and  $\{\mathbf{U}\}$  represents the elastic displacement and electric potential vector.

The elastic displacement, electric potential, stress and electric displacement fields in stress singularity region, are expressed by the following equations.

$$u_j(r, \theta, \phi) = b_j(\theta, \phi) r^{1-\lambda} \quad (16)$$

$$\psi(r, \theta, \phi) = q(\theta, \phi) r^{1-\lambda} \quad (23)$$

By differentiating the above two equations, get the angular function of strain and electric field equation respectively. The stress and electric displacement distribution equations in the stress singularity region can be expressed as follows.

$$\sigma_{ij}(r, \theta, \phi) = K_{ij} r^{-\lambda} f_{ij}(\theta, \phi) \quad \text{and}$$

$$d_i(r, \theta, \phi) = F_i r^{-\lambda} l_i(\theta, \phi) \quad (24)$$

Where  $r$  represents the distance from the stress singular point,  $b_j(\theta, \phi)$  the angular function of elastic displacement,  $q(\theta, \phi)$  the angular function of electric potential,  $f_{ij}(\theta, \phi)$  the angular function of stress distribution,  $l_i(\theta, \phi)$  the angular function of electric displacement,  $K_{ij}$  the intensity of singularity,  $F_i$  the intensity of electric field, and  $\lambda$  the order of stress singularity. Angular functions of stress and electric displacement components obtained from Eigen analysis in (22) are examined.

### 3. MODEL AND MATERIAL OF ANALYSIS

The model of 3D orthotropic piezoelectric bonded joints for eigenanalysis is shown in Fig. 2(a). The angle of  $\theta$  and  $\phi$  are  $180^\circ$  and  $90^\circ$ , respectively. In eigenanalysis, a mesh division for the joint is needed for the analysis. The mesh developed on  $\phi$ - $\theta$  plane is shown in Fig. 2(b), where the surface of a unit sphere is subdivided into  $\phi \times \theta = 10^\circ \times 10^\circ$  for rough mesh and  $\phi \times \theta = 2^\circ \times 2^\circ$  for fine mesh.

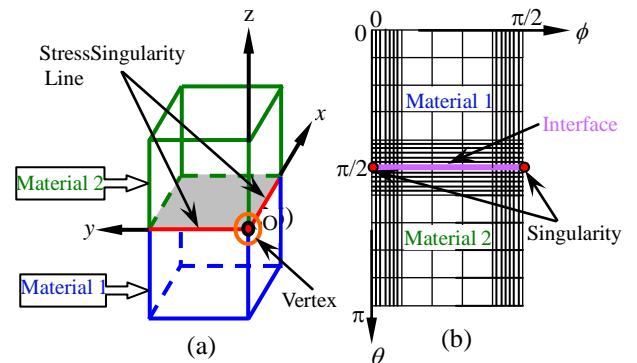


Fig.2:(a) 3D piezoelectric joints with corner in  $x, y, z$  co-ordinate, and (b) A mesh on the developed  $\phi$ - $\theta$  plane

The material properties of orthotropic piezoelectric materials are shown in the Table 1. PVDF(Polyvinylidene Fluoride)and BSN(Barium Sodium Niobate)are used for upper and lower materials in the analysis.

Table 1: Material properties for PVDF and BSN

Material	Elastic constant $10^{10}, \text{N/m}^2$								
	$C_{11}$	$C_{12}$	$C_{13}$	$C_{22}$	$C_{23}$	$C_{33}$	$C_{44}$	$C_{55}$	$C_{66}$
PVDF	0.361	0.161	0.142	0.313	0.131	0.163	0.055	0.059	0.069
BSN	23.9	10.4	5.0	24.7	5.2	13.5	6.5	6.6	7.6

Material	Piezoelectric constant, $(\text{C/m}^2)$					Dielectric constant $(10^{-10} \text{ C/Vm})$		
	$e_{15}$	$e_{24}$	$e_{31}$	$e_{32}$	$e_{33}$	$\chi_{11}$	$\chi_{22}$	$\chi_{33}$
PVDF	-0.01593	-0.01265	0.032075	-0.00407	-0.02119	5.4	6.64	5.93
BSN	2.8	3.4	-0.4	-0.3	4.3	196	201	28

#### 4. NUMERICAL RESULT AND DISCUSSION

Solving eigen equation yields many roots  $p$  and eigen vectors corresponding to each eigen value are obtained. However, if the root is within the range of  $0 < p < 1$ , this fact indicates that the stress field has singularity. The value of order of singularity at the singularity corner is 0.5787

In the present paper, the order of singularity is investigated varying the material constants. A ratio of material constants to a specified material constant is introduced as follows.

$$\frac{e}{e_n} = S, \quad \frac{\chi}{\chi_n} = S, \text{ and } \frac{c}{c_n} = S$$

Where  $e_n, \chi_n$  and  $c_n$  represent the referential piezoelectric, dielectric and elastic constants, respectively of PVDF and BSN.  $e, \chi$  and  $c$  represent the new piezoelectric, dielectric and elastic constants, respectively. The value of  $S$  varies from 0.0001 to 10000. To plot the value logarithmic value of the  $S$  is taken.

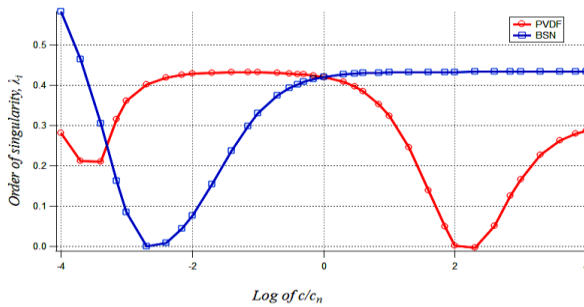


Fig. 3: Variation of order of singularity against  $c/c_n$

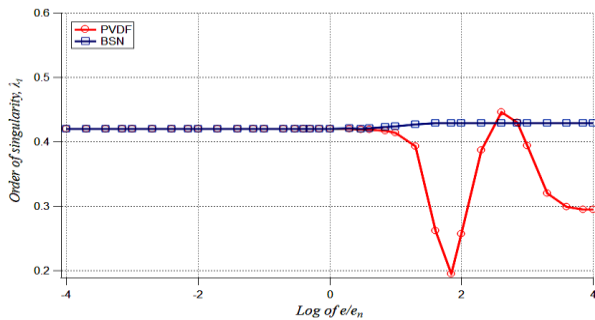


Fig. 4: Variation of order of singularity against  $e/e_n$

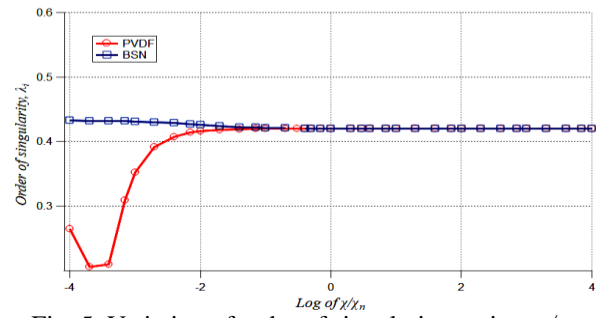


Fig. 5: Variation of order of singularity against  $\chi/\chi_n$

In these three graphs, it is seen that by changing elastic properties the order of singularity is changing significantly. But when changing the value of piezoelectric and di-electric properties of orthotropic material shows the small effect on the order of singularity. So it can be said that changing of elastic properties have the significant effect on singularity.

Angular functions obtained from eigen equation, Eq. (22), are examined. Distributions of angular function of elastic displacement and electric potential on a  $\theta-\phi$  plane are shown in Fig. 6~9 and angular function of stress and electric displacement are in shown in Figs. 10~ 15.

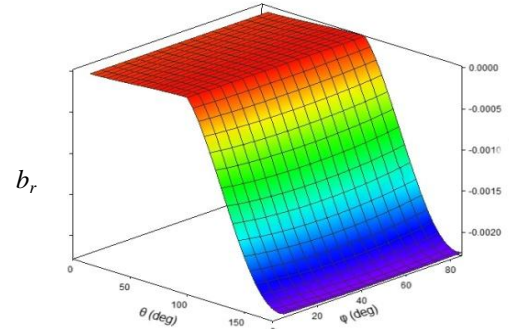


Fig 6: Distribution of angular function of displacement components  $b_r$ .

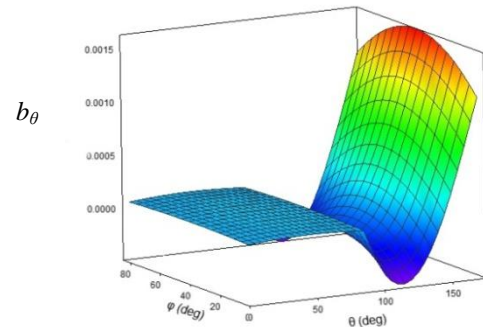


Fig 7: Distribution of angular function of displacement components  $b_\theta$ .

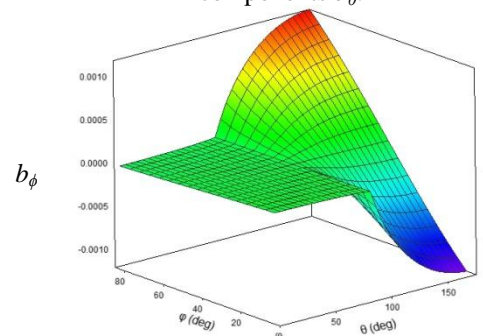


Fig. 8: Distribution of angular function of displacement components  $b_\phi$ .

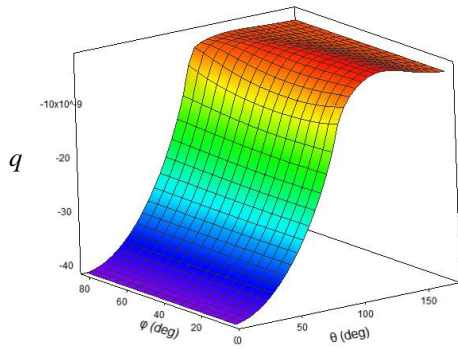


Fig. 9: Distribution of the angular function of electric potential  $q$ .

All of these graphs show that the angular functions are continuous at the interface. The interface of the joint is at  $\theta = 90^\circ$ .

Figures 10, 11 and 12 show the 3D distribution of angular function of stress in  $\phi$ - $\theta$  plane for  $\lambda = 0.5787$ . All these graphs show the angular function of stress has the higher value at the interface edge of the dissimilar material joint.

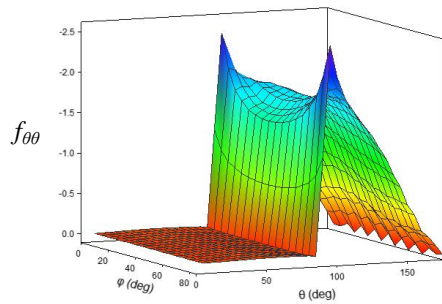


Fig. 10: Distribution of angular function of stress components  $f_{\theta\theta}$ .

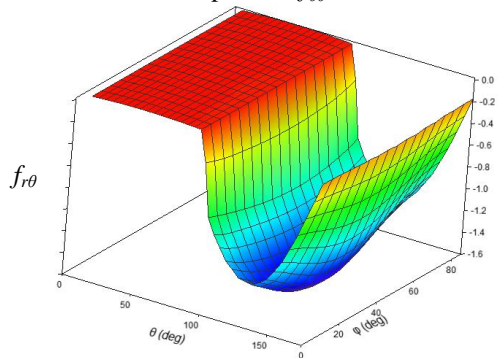


Fig. 11: Distribution of angular function of stress components  $f_{r\theta}$ .

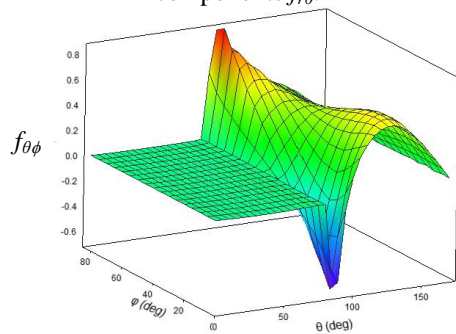


Fig. 12: Distribution of angular function of stress components  $f_{\theta\phi}$ .

Figures 13, 14 and 15 show the 3D distribution of angular function of electric displacement in  $\phi$ - $\theta$  plane for  $\lambda = 0.5787$ . All these graphs show the angular function of electric displacement is continuous at the interface of the dissimilar material joint.

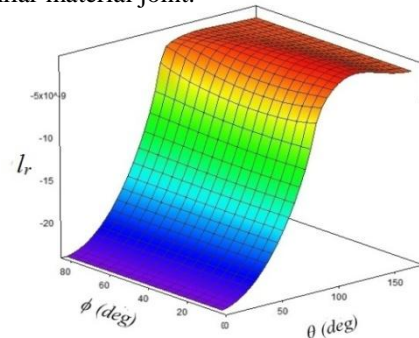


Fig. 13: Distribution of angular function of electric displacement components  $l_r$ .

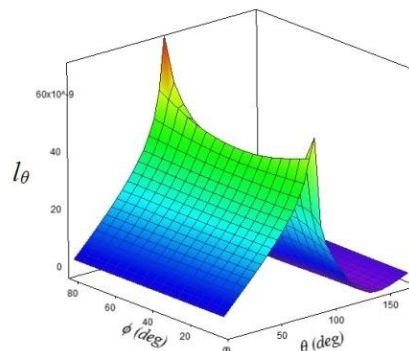


Fig. 14: Distribution of angular function of electric displacement components  $l_\theta$ .

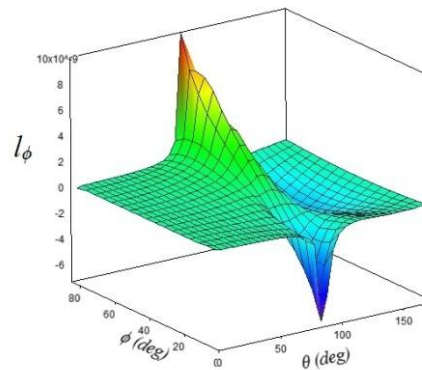


Fig. 15: Distribution of angular function of electric displacement components  $l_\phi$ .

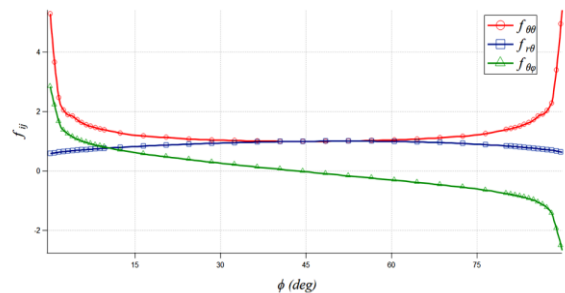


Fig. 16: Distribution of normalized angular function of stress components  $f_{ij}$  along  $\phi$  when  $\theta = 90^\circ$ .

The normalized angular function of stress is shown

in Fig.16 for  $\lambda = 0.5787$ . The angular function of stress against the angle  $\phi$  at  $\theta = 90^\circ$  is plotted. The stress singularity lines are at the free edge of the material joint. The graph shows that the value of stress increases rapidly near the free edge than the inner portion of the joints. The value of  $f_r$  and  $f_\theta$  is one and  $f_\phi$  is zero near  $\phi = 45^\circ$ . After that the values of angular function of stress are increased. Near free edge of the joint has the highest value of angular function. So there is a possibility of debonding and delamination occurs near the interface edge of the joint.

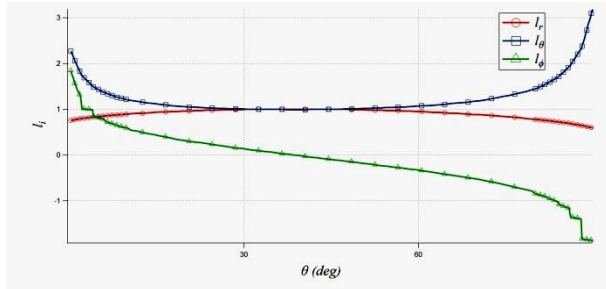


Fig. 17: Distribution of normalized angular function of electrical displacements components  $l_i$  along  $\phi$  when  $\theta = 90^\circ$

The normalized angular function of electric displacement is shown in fig. 17 for  $\lambda = 0.5787$ . The angular function of electric displacement against the angle  $\phi$  at  $\theta = 90^\circ$  is plotted. The shape of the curve is same as angular function of stress curve. The graph also shows that the value of electric displacement increases rapidly near the free edge than the inner portion of the joints. The value of  $l_r$  and  $l_\phi$  is one and  $l_\theta$  is zero near  $\phi = 45^\circ$ . After that the values of angular function of electric displacement are increased.

## 5. CONCLUSION

An eigen analysis near the vertex of orthotropic piezoelectric dissimilar joint was presented. Angular functions for stress and electric displacement at singularity corner were derived from eigen analysis using a finite element method. From the simulation results, the following conclusions can be drawn for the Orthotropic piezoelectric material joints.

- Elastic constant affects the order of singularity more significantly.
- Larger value of the angular function of stress and electric displacement occurs at the interface edge than the inner portion of the joint.
- It is suggested that debonding and crack of the interface may occur near the interface edge of the joints.

## 6. REFERENCES

- M. S. Islam and K. Hideo, "Investigation of Order of Singularity in 3D Transversely Isotropic Piezoelectric Bimaterial Joints by FEM", *Journal of Circuits, Systems, and Computers*, World Scientific Publishing Company, vol. 24, no. 2, pp. 1540001-21, 2014.
- <https://en.wikipedia.org/wiki/Piezoelectricity>
- [https://en.wikipedia.org/wiki/Adhesive\\_bonding](https://en.wikipedia.org/wiki/Adhesive_bonding)

- Md. Shahidul Islam and Koguchi Hideo, "Characteristics of singular stress distribution at a vertex in transversely isotropic piezoelectric dissimilar material joints", *Journal of Solid Mechanics and Materials Engineering*, vol. 4, issue 7, pp. 1011-1026, 2010.
- H. Koguchi, "Stress singularity analysis in three-dimensional bonded structure," *Trans. JSME A* 72, no. 724, pp. 2058-2065, 2006.
- J. Q. XU, and Y. Mutoh, "Singularity at the interface edge of bonded transversely isotropic piezoelectric dissimilar material", *JSME International Journal*, Series A, Vol.44, No. 4, 2001.
- T. Ikeda, H. Hirai, M. Abe, M. Chiba, and N. Miyazaki, "Stress intensity factor analysis of an interfacial corner between piezoelectric biomaterials in a two dimensional structure using H-integral Method," *Proceedings of the ASME, InterPACK*, pp.1-9, 2011.

## 7. NOMENCLATURE

Symbol	Meaning	Unit
$\sigma_{ij}$	Stress tensor	MPa
$d_i$	Electric displacement vector	C/m <sup>2</sup>
$\epsilon_{kl}$	Strain tensor	m/m
$E_k$	Electric field	N/C
$c_{ijkl}$	Elastic constant	N/m <sup>2</sup>
$e_{kij}$ ( $e_{ikl}$ )	Piezoelectric constant	C/m <sup>2</sup>
$\chi_{ik}$	Electric permittivity (dielectric constant)	C/Vm
$u_i$	Elastic displacement	m
$\phi$	Electric potential	V